Direct observation of the magnetic domain evolution stimulated by temperature and magnetic field in PrMnGeSi alloy

S. L. Zuo, B. Zhang, K. M. Qiao, L. C. Peng, R. Li, J. F. Xiong, Y. Zhang, X. Zhao, D. Liu, T. Y. Zhao, J. R. Sun, F. X. Hu, Y. Zhang, and B. G. Shen

Citation: AIP Advances **8**, 056801 (2018); doi: 10.1063/1.5006385
View online: https://doi.org/10.1063/1.5006385
View Table of Contents: http://aip.scitation.org/toc/adv/8/5
Published by the American Institute of Physics

AIP ADVANCES **8**, 056801 (2018)

Direct observation of the magnetic domain evolution stimulated by temperature and magnetic field in PrMnGeSi alloy

S. L. Zuo,[1,2] B. Zhang,[1,2] K. M. Qiao,[1,2] L. C. Peng,[1,2] R. Li,[1,2] J. F. Xiong,[1,2] Y. Zhang,[1,2] X. Zhao,[1,2] D. Liu,[1,2] T. Y. Zhao,[1] J. R. Sun,[1,2] F. X. Hu,[1,2] Y. Zhang,[1,a] and B. G. Shen[1,2,a]

[1]*State Key Laboratory for Magnetism, Institute of Physics, Chinese Academy of Sciences, Beijing 100190, P. R. China*

[2]*University of Chinese Academy of Sciences, Beijing, 100049, P. R. China*

(Presented 8 November 2017; received 25 September 2017; accepted 10 October 2017; published online 6 December 2017)

The magnetic domain evolution behavior under external field stimuli of temperature and magnetic field in $PrMn_2Ge_{0.4}Si_{1.6}$ compound is investigated using Lorentz transmission electron microscopy. A spontaneous 180° magnetic domain is observed at room temperature and it changes with temperature. Dynamic magnetization process is related to the rotation of magnetic moments, resulting in the transforming of magnetic domains from 180° type to a uniform ferromagnetic state with almost no pinning effects under the in-plane magnetic field at room temperature. X-ray powder diffraction is performed on $PrMn_2Ge_{0.4}Si_{1.6}$ at different temperatures to study the temperature dependence of crystal structure and lattice parameter.
https://doi.org/10.1063/1.5006385

I. INTRODUCTION

The studies of RMn_2X_2 (R is a rare earth and X is Si or Ge) compounds have attracted a great deal of attentions due to their layered crystal structure and interesting physical phenomena, such as coupled magnetic and crystallographic transitions or valence-related transitions, superconductivity, heavy fermion and Kondo behaviour.[1–7] The RMn_2X_2 alloys have a body centered tetragonal $ThCr_2Si_2$-type structure with space group *I*4/*mmm* and exhibit a vast variety of magnetic structures and magnetic phase transitions with temperature, mechanical pressure or magnetic field[8–10] due to the fact that the magnetic states of Mn-sublattice are sensitive to the inter-planar and intra-planar Mn–Mn distances.[11–14] Four magnetic transitions are observed in pure $PrMn_2Ge_2$ phase below 500 K[15,16] while one relatively simple antiferromagnetic transition exist below 368 K in $PrMn_2Si_2$.[17] The substitution of Si for Ge leads to a linear decrease of the lattice constants and the magnetic state changes from the ferromagnetic ordering of $PrMn_2Ge_2$ to the antiferromagnetic ordering of $PrMn_2Si_2$ at room temperature due to the atomic size difference between Si and Ge.[16]

The magnetic behaviors of $PrMn_2Ge_{2-x}Si_x$ (x=0-2) compounds are governed by the strong dependence of the magnetic couplings on the Mn–Mn spacing, resulting different magnetic states due to compositional dependence of lattice parameters.[16,18,19] For example, antiferromagnetism exits in the samples with x >1.6 and the re-entrant ferromagnetism with co-existence of canted ferromagnetism and antiferromagnetism is observed in the cases of x = 1.2 or 1.3 below the magnetic transition temperature.[16,18] Although the crystal structure and magnetic properties of various $PrMn_2Ge_{2-x}Si_x$ (x = 0–2) compounds have been investigated by X-ray powder diffraction, AC susceptibility, differential

[a]Corresponding author. Electronic mail: shenbaogen@yeah.net; zhangy@iphy.ac.cn

scanning calorimetry, and Neutron diffraction, the detailed magnetic domain evolution near the phase transition remain elusive.[16,18]

Two magnetic phase transitions above room temperature and a canted antiferromagnetic structure at room temperature are expected in $PrMn_2Ge_{0.4}Si_{1.6}$ based on previous report.[18] Although the magnetic transition is evident in magnetic measurements at ~282 K, no ferromagnetic component is detected below 282 K from the neutron diffraction patterns,[18] similar to $PrMn_{1.2}Fe_{0.8}Ge_2$.[20,21] Thus, studying the magnetic domain structures during in-situ magnetization and phase transformation will provide a fruitful playground for the exploration of fundamental physics of this anomaly phenomenon. In this study, the evolution of the magnetic domains and the crystal structures induced by temperature are investigated in $PrMn_2Ge_{0.4}Si_{1.6}$ alloy by means of in situ Lorentz transmission electron microscopy (LTEM) and X-ray diffraction, respectively. Moreover, the dynamic behavior of the magnetic domain walls under the in-plane magnetic field is demonstrated at room temperature using LTEM providing enhanced understanding of magnetic phases in $PrMn_2Ge_{0.4}Si_{1.6}$ alloy.

II. EXPERIMENTAL

Polycrystalline $PrMn_2Ge_{0.4}Si_{1.6}$ is prepared by arc melting technique in high-purity argon atmosphere. The thin plate for LTEM observation is cut from the polycrystalline ingot and thinned by mechanical polishing and argon ion milling. The details of the preparation and other magnetic properties will be reported elsewhere. To image the magnetic domain configuration, a JEOL-dedicated LTEM is used with almost no remnant magnetic field around the sample. In situ TEM observations of magnetic domain evolution under external fields are conducted using a liquid-nitrogen TEM sample holder (100–300 K) and an in-plane magnetization holder. With the use of the Fresnel LTEM method, the magnetic domain walls can be imaged as bright contrast (converge beam) or dark contrast (diverge beam). The high-resolution in-plane magnetization distribution map is obtained using the commercial QPt software based on the transport of the intensity equation (TIE). The magnetic properties are measured by a superconducting quantum interference magnetometer (SQUID-VSM). The crystal structure of the samples is checked by X-ray powder equipped with Cu-Kα radiation over the temperature range 4–300 K.

III. RESULTS AND DISCUSSION

The temperature dependence of magnetization in an external field of 10 mT for $PrMn_2Ge_{0.4}Si_{1.6}$ is shown in Fig. 1(a). The change of magnetization is obvious as the temperature decreases, consistent with previous results.[18] A strong splitting between zero field-cooled (ZFC) and field-cooled (FC) magnetizations is observed, which may result from the occurrence of different domain configurations due to the external magnetic field-induced reorientation to the ferromagnetic components, similar to $Pr_{1-x}Tb_xMn_2Ge_2$ with $x \leq 0.6$ and $La_{1-x}R_xMn_2Si_2$.[22,23] The $1/\chi$–T (inversion of susceptibility versus temperature) indicates notable ferromagnetism near room temperature. Moreover, the magnetic hysteresis behavior is detected as shown in the inset of Fig. 1(b). Such features could be interpreted due to the presence of ferromagnetism. X-ray diffraction patterns for $PrMn_2Ge_{0.4}Si_{1.6}$ at selected temperatures are shown in Fig. 1(c), and the temperature dependence of lattice constant a derived from X-ray diffraction patterns exhibits non-linear behavior shown in Fig. 1(d). It can be seen that the lattice constants at high temperatures are larger than 4.06 Å, which roughly indicates that the interlayer coupling of Mn is ferromagnetic. The magnetic coupling is expected to be antiferromagnetic when the lattice constant is smaller than 4.06 Å. This behavior corresponds well with the anomaly change of the M–T curve (Fig. 1(a)), which may indicate strong coupling between the magnetism and the crystal lattice.[16,18,24]

Under the isothermal condition, magnetic entropy change can be calculated by Maxwell relation of: $\Delta S_M = \int_0^H \frac{\partial M}{\partial T} dH$. The temperature dependence of ΔS_M for $PrMn_2Ge_{0.4}Si_{1.6}$ compound is shown in Fig. 2. A large peak around room temperature is clearly indicated. According to the characteristic of M–T curve, the value of dM/dT is positive within the range of 120–250 K. As a result, positive ΔS_M is observed within a large range of temperature, which can be kept even

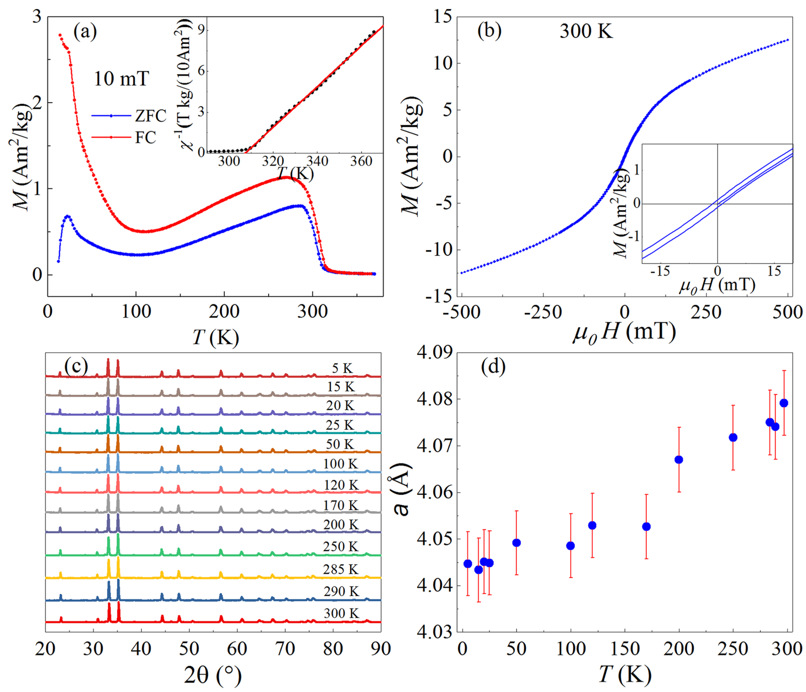

FIG. 1. (a) Temperature dependence of the magnetization (M–T curve) measured in an applied field of 10 mT. Inset shows the $1/\chi$–T (inversion of susceptibility versus temperature) and the Curie–Weiss fitting (red line). (b) Magnetization vs. field (M–H curve) measurement at 300 K. The magnetic loop near the zero magnetic fields is enlarged shown in the inset. (c) X-ray diffraction patterns at selected temperatures. (d) Temperature dependence of lattice constant a.

the field change is as high as 0–5 T, indicating the antiferromagnetic ground state. These results imply that $PrMn_2Ge_{0.4}Si_{1.6}$ compound is ferromagnetic ordered state at room temperature and it undergoes a magnetic phase transition from ferromagnetism to antiferromagnetism while lowering temperature.

The in-situ cooling experiment from 290 to 125 K is displayed in Figure 3. At room temperature, a spontaneous 180° magnetic domain structure with a periodicity of ~ 300 nm is observed (Fig. 3(a)) with the corresponding in-plane spin texture obtained by TIE shown in Fig. 3(b), where the blue and red regions correspond to anti-parallel magnetization distribution. When decreasing the temperature, the magnetic domains broaden first (Fig. 3(c)) and then break at the locations where the domains narrow faster as shown in Fig. 3(d) and 3(e). Simultaneously, the magnetic domains begin to disappear in an order from the top of the viewed area. As the temperature decreases further, the magnetic domains

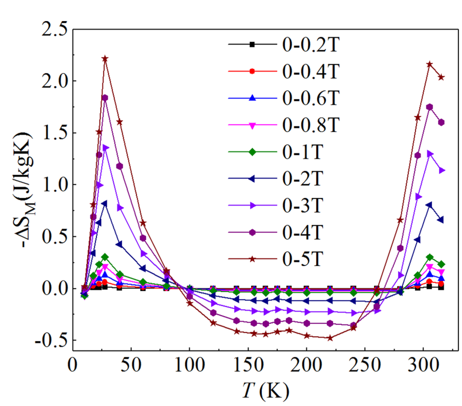

FIG. 2. Temperature dependences of ΔS_M at different applied magnetic field change intervals for $PrMn_2Ge_{0.4}Si_{1.6}$.

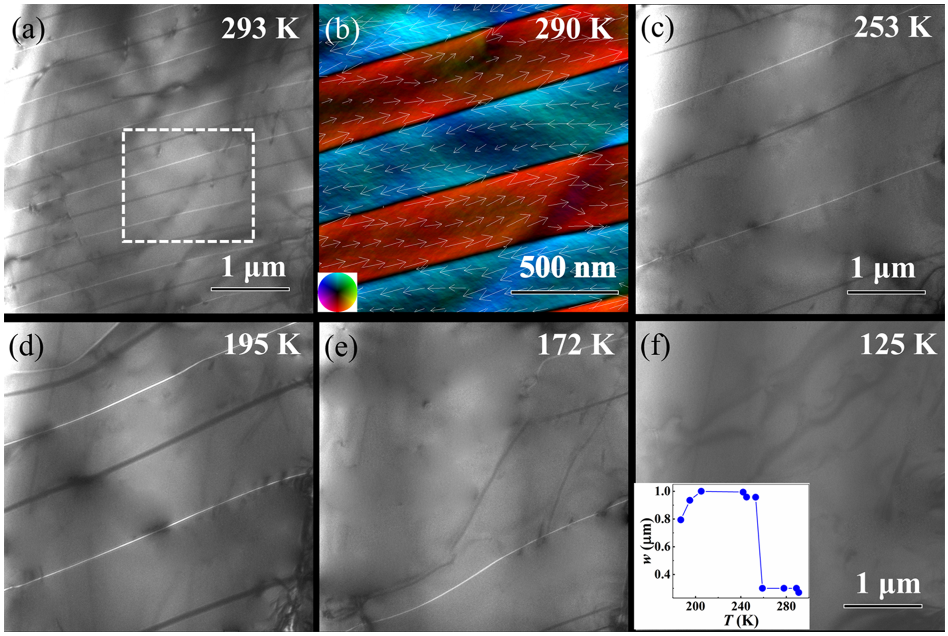

FIG. 3. Under-focused LTEM images for the temperature dependence of magnetic domain evolution in $PrMn_2Ge_{0.4}Si_{1.6}$. (a) The spontaneous magnetic domains at 290 K and (b) the corresponding in-plane magnetic textures obtained by TIE analysis with the magnitude and orientation of the magnetization depicted by arrows and the colors for the selected rectangle area. (c)–(f) Magnetic domain evolution as the temperature decreases from 253 to 125 K. The temperature dependence of magnetic domain width is summarized in the inset of (f).

completely disappear and a uniform contrast is formed (Fig. 3(f)). The inset of Fig. 3(f) summarizes the temperature dependence of domain width based on the LTEM images of Fig. 3. The characteristics of the magnetic domain change is similar to a magnetic transition from a ferromagnetism to an antiferromagnetism.[18,19,22–25] The anomaly detected in the magnetization measurements about 280 K (Fig. 1(a)) may be caused by the presence of ferromagnetic phase around room temperature.[22,26] As temperature decreases, ferromagnetic components reduce due to the ferromagnetic-antiferromagnetic transition[25,27] and resulting in the change of magnetic domain structure shown in Fig. 3.

Finally, we try to observe the magnetization dynamics through the domain wall motion driven by in-plane magnetic field. The magnetization process accompanied by annihilation and nucleation of domain walls has been captured by in situ LTEM at room temperature. The magnetic domain evolution under an in-plane magnetic field is shown in Fig. 4. The magnetic domain is scrutinized before switching on the magnetic field (Fig. 4(a)) and the magnetization directions are indicated by red and white arrows. As the magnetic field is increased, domain wall motion is initiated and the domains with the magnetic moment aligning along the red arrow become large and the area fraction of the opposite domains is reduced as shown in Fig. 4(b). While further increasing the magnetic field, the domains with the direction of white arrow release from the grain boundary, shrink to the center of the sample (Fig. 4(c)) and then disappear at 16.6 mT (Fig. 4(d)). The magnetic field dependence of the domain width along the white arrow direction is summarized in the inset of Fig. 4(e) based on the LTEM observation, which shows the domain width decreases as the magnetic field increase. The magnetic domains totally disappear into a uniform contrast as the magnetic field is increased to 25.3 mT as shown in Fig. 4(e), which correspond to a saturated magnetization state. The reduction of the magnetic field is necessary to study the domain nucleation. As the magnetic field is decreased to 16.7 mT after saturation, the magnetic domain nucleates at the marked location in Fig. 4(f). The domain wall prefers to initiate nucleation from the middle of the sample similar to the position where the domain walls disappear lastly. Little pining at boundaries are observed during the magnetization and a relative low magnetic field of 25.3 mT can saturate the sample magnetization, which consists with the feature of *M*–*H* curve with low coercivity.

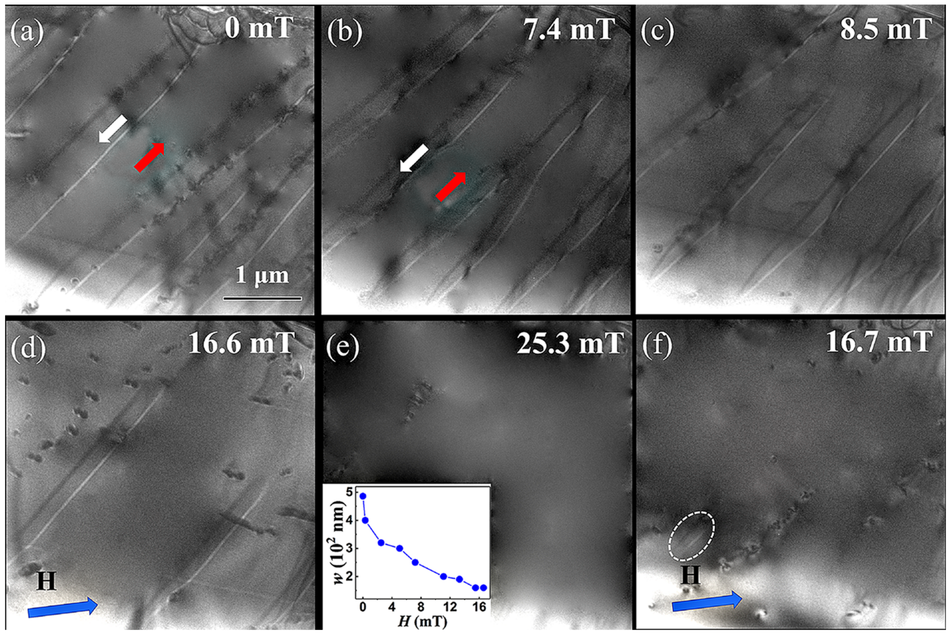

FIG. 4. Real-space LTEM images showing the magnetic field dependence of magnetic domain evolution in $PrMn_2Ge_{0.4}Si_{1.6}$ at room temperature. Under-focused LTEM images recorded by increasing the in-plane magnetic field to (a) 0, (b) 7.4, (c) 8.5, (d) 16.6, (e) 25.3 mT, and then decreasing magnetic field to (f) 16.7 mT. The inset of (e) summarizes the width change of magnetic domain with the magnetic moment aligning along the white arrow direction under the magnetic fields. The magnetic domain is marked out with a white ellipse in (f). The red and white arrows indicate magnetization direction. The direction of the in-plane magnetic field is indicated by a blue arrow.

IV. CONCLUSIONS

In summary, magnetic domain evolutions under the stimuli of the temperature and in-plane magnetic field are clearly demonstrated in $PrMn_2Ge_{0.4}Si_{1.6}$ alloy via real-space LTEM imaging. The spontaneous 180° magnetic domain is observed at room temperature due to the presence of ferromagnetism. The magnetic domains significantly change with decreasing temperature and disappear at low temperature. Moreover, little pinning is observed during magnetization process, which may associate to the characteristic of ferromagnetic state at room temperature and accord with the magnetization curve.

ACKNOWLEDGMENTS

This work was supported by the National Basic Research Program of China (Grant No. 2014CB643702) and the National Key Research and Development Program of China (Grant No. 2016YFB0700902, 2016YFB0700903) and the National Natural Science Foundation of China (Grant No. 51590880, 11374349). The Knowledge Innovation Project of the Chinese Academy of Sciences (Grant No. KJZD-EW-M05) and the Youth Innovation Promotion Association, CAS, 2015004.

[1] A. Szytuła, Handbook of Magnetic Materials **6**, 85 (1991).
[2] J. L. Wang, S. J. Campbell, A. J. Studer, M. Avdeev, R. Zeng, and S. X. Dou, J. Phys.: Condens. Matter **21**, 124217 (2009).
[3] T. Fujiwara, H. Fujii, and T. Shigeoka, Phys. Rev. B **63**, 174440 (2001).
[4] S. Chaudhary, M. K. Chattopadhyay, K. J. Singh, S. B. Roy, P. Chaddah, and E. V. Sampathkumaran, Phys. Rev. B **66**, 014424 (2002).
[5] M. Hofmann, S. J. Campbell, and A. V. J. Edge, Phys. Rev. B **69**, 174432 (2004).
[6] A. M. Bebb, J. W. Taylor, J. A. Duffy, Z. F. Banfield, M. J. Cooper, M. R. Lees, J. E. McCarthy, and D. N. Timms, Phys. Rev. B **71**, 024407 (2005).
[7] E. G. Gerasimov, N. V. Mushnikov, and T. Goto, Phys. Rev. B **72**, 064446 (2005).
[8] J. H. V. J. Brabers, K. H. J. Buschow, and F. R. de Boer, Phys. Rev. B **59**, 9314 (1999).
[9] R. Welter and B. Malaman, J. Alloys Compd. **354**, 35 (2003).
[10] M. F. M. Din, J. L. Wang, S. J. Campbell, R. Zeng, W. D. Hutchison, M. Avdeev, S. J. Kennedy, and S. X. Dou, J. Phys. D: Appl. Phys. **46**, 445002 (2013).

[11] A. Szytula and J. Leciejewicz, *Handbook on Crystal Structures and Magnetic Properties of Rare Earth Intermetallics* (FL: CRC Press, Boca Raton, 1994).
[12] G. Venturini, B. Malaman, and E. Ressouche, J. Alloys Compd. **240**, 139 (1996).
[13] G. Venturini, R. Welter, E. Ressouche, and B. Malaman, J. Magn. Magn. Mater. **150**, 197 (1995).
[14] J. S. Lord, P. C. Riedi, G. J. Tomka, C. Kapusta, and K. H. J. Buschow, Phys. Rev. B **53**, 283 (1995).
[15] I. Nowik, Y. Levi, I. Felner, and E. R. Bauminger, J. Magn.Magn. Mater. **147**, 373 (1995).
[16] S. Kervan, A. Kilic, and A. Gencer, J. Phys.: Condens. Matter **16**, 4955 (2004).
[17] R. Welter, G. Venturini, D. Fruchard, and B. Malaman, J. Alloys Compd. **191**, 263 (1993).
[18] J. L. Wang, S. J. Campbell, M. Hofmann, S. J. Kennedy, R. Zeng, M. F. M. Din, S. X. Dou, A. Arulraj, and N. Stusser, J. Phys.: Condens. Matter **25**, 386003 (2013).
[19] J. L. Wang, S. J. Kennedy, S. J. Campbell, M. Hofmann, and S. X. Dou, Phys. Rev. B **87**, 104401 (2013).
[20] J. L. Wang, S. J. Campbell, J. M. Cadogan, O. Tegus, A. J. Studer, and M. Hofmann, J. Phys.: Condens. Matter **18**, 189 (2006).
[21] J. L. Wang, A. J. Studer, S. J. Campbell, M. Hofmann, and J. M. Cadogan, Physica B **385**, 326 (2006).
[22] E. Duman, M. Acet, Y. Elerman, A. Elmali, and E. F. Wassermann, J. Magn. Magn. Mater. **238**, 11 (2002).
[23] E. Duman, M. Acet, I. Dincer, A. Elmali, and Y. Elerman, J. Magn. Magn. Mater. **309**, 40 (2007).
[24] I. Dincer, Y. Elerman, A. Elmali, H. Ehrenberg, H. Fuess, and C. Baehtz, Solid State Commun. **140**, 245 (2006).
[25] Y. Murakami, J. H. Yoo, D. Shindo, T. Atou, and M. Kikuchi, Nature **423**, 965 (2003).
[26] E. Duman, M. Acet, I. Dincer, A. Elmali, and Y. Elerman, J. Magn. Magn. Mater. **529**, 272 (2004).
[27] J. Q. He, V. V. Volkov, T. Asaka, S. Chaudhuri, R. C. Budhani, and Y. Zhu, Phys. Rev. B **82**, 224404 (2010).